



---

# Comparison of Flow-induced Crystallization Melt Spinning Processes

S.S.N. Perera

Department of Mathematics, University of Colombo, Colombo 03, Sri Lanka

Correspondence: [ssnp@maths.cmb.ac.lk](mailto:ssnp@maths.cmb.ac.lk)

**Abstract.** The melt spinning process for artificial fibers has been studied by many research groups throughout the world during the last four decades. However, comparison of flow-induced crystallization melt spinning processes has not yet been treated in the literature. In this study, we analyse the dynamics of the flow induced crystallization melt spinning process. Further, we study the sensitivity of the process with respect to fluid shear modulus. Non-Newtonian and Maxwell-Oldroyd models are used to describe the rheology of the polymer the fiber is made of. It has been found that the flow-induced crystallization Maxwell-Oldroyd model has an upper bound for the final velocity.

**Key words:** Fiber spinning, Non-Newtonian, Maxwell-Oldroyd

---

## 1. Introduction

The fiber spinning process is used to make all types of synthetic textile fibers (nylon, polyester, rayon, etc.). In the melt spinning version of the process, molten polymer is extruded a die called a spinneret to create a thin long fiber. Far away from the spinneret, the fiber is wrapped around a drum, which pulls it away at a pre-determined take-up speed. The take-up speed is much higher than the extrusion speed; in industrial processes the take-up speed is about 50m/s and the extrusion speed is about 10m/s, see (2, 4). The ratio between the take-up speed  $v_L$  and the extrusion speed  $v_0$  is called draw-ratio and denoted by  $d = v_L/v_0 > 1$  and hence the filament is stretched considerably in length and therefore decreases in diameter. The ambient atmosphere temperature is below the polymer solidification temperature such that the polymer is cooled and solidifies before the take-up, see Figure 1. In industrial processes a whole bundle of hundreds of single filaments is extruded and spun in parallel, however for the analysis we consider a single filament.

The dynamics of melt spinning processes has been studied by many research groups throughout the world during the last decades starting with the early works of Kase and Matsuo (3) and Ziabicki (10). Despite great scientific progress in the dynamics of fiber formation processes, especially in flow induced crystallization process, there are still some unsettled issues. For example, comparison of flow-induced crystallization melt spinning processes has not yet been treated in the literature. The sensitivity of the Maxwell-Oldroyd model (both isothermal and non-isothermal) with respect to the characteristic relaxation

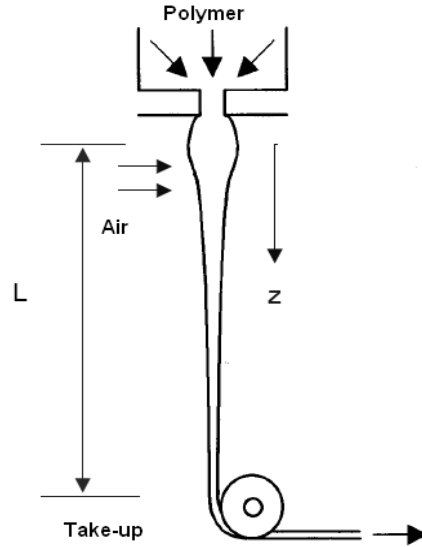


**Figure 1** Sketch of the melt spinning process.

time has been discussed in the literature without considering the crystallization process (7, 8). To investigate the same concept with the crystallization process is quite interesting from both the theoretical and industrial points of view because it is closely related to high quality control of products and its theoretical analysis involves the fundamental understanding of the nonlinear dynamics of the process. In this study, we analyse the behaviour of the flow induced crystallization melt spinning process using non-Newtonian and Maxwell-Oldroyd models. Further, we study the sensitivity of the flow induced crystallization process with respect to the fluid shear modulus.

## 2. Melt Spinning Models

Considering the basic conservation laws for the mass, momentum and energy of the viscous polymer jet, one can obtain the following set of equations, by averaging over the cross-section of the slender fiber, see (4, 5, 6, 7).

$$\rho Av = W_0 . \quad (1a)$$

$$\rho Av \frac{dv}{dz} = \frac{dA\tau}{dz} - \sqrt{\frac{A}{\pi}} C_d \rho_{air} v^2 + \rho Ag , \quad (1b)$$

$$\rho C_p v \frac{dT}{dz} = -\frac{2\alpha\sqrt{\pi}}{\sqrt{A}} (T - T_\infty) + \rho \Delta H v \frac{d\phi}{dz} , \quad (1c)$$

In the mass balance (1a),  $A$  denotes the cross-sectional area of the fiber, and  $v$  is the velocity of the fiber along the spinline. The density  $\rho$  of the polymer is assumed to be constant. In the momentum balance (1b),  $z$  denotes the coordinate along the spinline and the axial stress  $\tau$  is related via the constitutive equations (for the non-Newtonian case equation (1d) and the Maxwell-Oldroyd case equation (1e))

$$\tau = 3\eta \frac{dv}{dz} , \quad (1d)$$

$$\tau + \lambda \left( v \frac{d\tau}{dz} - 2\tau \frac{dv}{dz} \right) = 3\eta \frac{dv}{dz} \quad (1e)$$

to the viscosity  $\eta$  and characteristic relaxation time  $\lambda$ .

In the energy equation (1c),  $T$  and  $C_p$  denote the temperature and the heat capacity of the polymer,  $T_\infty$  is the temperature of the quench air and  $\alpha$  denotes the heat transfer coefficient between the fiber and the quench air.

According to (4), we assume the following relation for the heat transfer coefficient

$$\alpha = \frac{0.21}{R_0} \kappa \text{Re}_{\text{air}}^{\frac{1}{3}} \left[ 1 + \frac{64v_c^2}{v^2} \right]^{\frac{1}{6}}$$

depending on the Reynolds-number of the quench air flow

$$\text{Re}_{\text{air}} = \frac{2v\rho_{\text{air}}}{\eta_{\text{air}}} \sqrt{\frac{A}{\pi}}$$

Here  $R_0$  is the radius of the spinneret,  $\rho_{\text{air}}$ ,  $\eta_{\text{air}}$  and  $\kappa$  represent respectively the density, viscosity and heat conductivity of the air and  $v_c$  is the velocity of the quench air.

The crystallization process generates an enthalpy by change and this is represented by third term of the equation (1c) and  $\Delta H$  is the specific heat of fusion of a perfect crystal and  $\phi$  is the degree of crystallinity. According to (4), the model for the evolution of  $\phi$  is given by

$$v \frac{d\phi}{dz} = (\phi_\infty - \phi) K_{\text{max}} \exp \left[ -4 \ln 2 \left( \frac{T - T_{\text{max}}}{D} \right)^2 \right]. \quad (1f)$$

Here  $\phi_\infty$  is the ultimate crystallinity,  $K_{\text{max}}$  the maximum crystallization rate,  $T_{\text{max}}$  the fluid temperature having the maximum crystallization rate and  $D$  denotes the crystallization half width temperature range.

The viscosity and characteristic relaxation time are given by

$$\eta = \eta_0 \exp \left[ \frac{E_a}{R_G} \left( \frac{1}{T} - \frac{1}{T_0} \right) \right], \quad (1g)$$

$$\lambda = \lambda_0 \exp \left[ \frac{E_a}{R_G} \left( \frac{1}{T} - \frac{1}{T_0} \right) \right]. \quad (1h)$$

Here  $\eta_0 > 0$  is the zero shear viscosity at the initial temperature  $T_0$ ,  $E_a$  denotes the activation energy,  $R_G$  is equal to the gas constant and  $\lambda_0 = \frac{\eta_0}{G}$  ( $G$  is the fluid shear modulus).

The system (1) is subject to the boundary conditions

$$v = v_0 \quad T = T_0 \quad \phi = 0 \quad \text{at } z = 0 \quad (1i)$$

$$v = v_L \quad \text{at } z = L \quad (1j)$$

where  $L$  denotes the length of the spinline.

### 3. Dimensionless Form

Introducing the dimensionless quantities

$$z^* = \frac{z}{L}, \quad v^* = \frac{v}{v_0}, \quad z^* = \frac{z}{L}, \quad T^* = \frac{T}{T_0}, \quad A^* = \frac{A}{A_0}, \quad \tau^* = \frac{\tau L}{\eta_0 v_0}, \quad \phi^* = \frac{\phi}{\phi_\infty},$$

the system (1) can be formulated in dimensionless form. Dropping the star and considering the non-Newtonian and Maxwell-Oldroyd cases the system can be presented as follows

$$\frac{dv}{dz} = \frac{\tau}{3\eta}, \quad (2a)$$

$$\frac{d\tau}{dz} = \text{Re} \left( \frac{1}{3\eta} v\tau - \text{Fr}^{-1} + C_1 v^{\frac{5}{2}} \right) + \frac{1}{3\eta} \frac{\tau^2}{v}, \quad (2b)$$

$$\frac{dT}{dz} = -C_2 \frac{(T - T_\infty)}{\sqrt{v}} + \frac{\Delta H \phi_\infty}{T_0 C_p} \frac{d\phi}{dz}, \quad (2c)$$

$$\frac{d\phi}{dz} = \frac{K_{max} L}{v_0} \left( \frac{1 - \phi}{v} \right) \exp \left[ -4 \ln 2 \left( \frac{T - T_{max}}{D} \right)^2 \right]. \quad (2d)$$

$$\text{Re} v \frac{dv}{dz} = \frac{d\tau}{dz} - \frac{\tau}{v} \frac{dv}{dz} + \text{Re} \left( \text{Fr}^{-1} - C_1 v^{\frac{5}{2}} \right), \quad (3a)$$

$$3\eta \frac{dv}{dz} = \tau + \text{De} \left( v \frac{d\tau}{dz} - 2\tau \frac{dv}{dz} \right), \quad (3b)$$

$$\frac{dT}{dz} = -C_2 \frac{(T - T_\infty)}{\sqrt{v}} + \frac{\Delta H \phi_\infty}{T_0 C_p} \frac{d\phi}{dz}, \quad (3c)$$

$$\frac{d\phi}{dz} = \frac{K_{max} L}{v_0} \left( \frac{1 - \phi}{v} \right) \exp \left[ -4 \ln 2 \left( \frac{T - T_{max}}{D} \right)^2 \right]. \quad (3d)$$

In system (2) and (3),  $\text{Re} = \frac{\rho L v_0}{\eta_0}$  is the Reynolds number,  $\text{Fr}^{-1} = \frac{g L}{v_0^2}$  is the inverse of the Froude number,  $C_1 = \frac{C_d \rho_{air} L \sqrt{\pi}}{\rho \sqrt{A_0}}$  is the scaled drag coefficient and  $C_2 = \frac{2\alpha L \sqrt{\pi}}{\rho C_p v_0 \sqrt{A_0}}$  denotes the scaled heat transfer coefficient. The Deborah number De is given by

$$\text{De} = \frac{\lambda_0 v_0}{L} \exp \left[ \frac{E_a}{R_G T_0} \left( \frac{1}{T} - 1 \right) \right].$$

The systems (2) and (3), are subject to the boundary conditions

$$v(0) = 1 \quad T(0) = 1 \quad \text{and} \quad \phi(0) = 0, \\ v(1) = d,$$

where  $d$  is the draw ratio.

## 4. Numerical Results

### 4.1. Numerics

Both systems ((2) and (3)) of ODE are solved using the Matlab routine ode23tb. This routine uses an implicit method with backward differentiation to solve stiff differential equations. It is an implementation of TR-BDF2 (9), an implicit two stage Runge-Kutta formula where the first stage is a trapezoidal rule step and the second stage is a backward differentiation formula of order two.

Since both systems are boundary value problems, the shooting method is used to solve them.

### 4.2. Shooting Method

Now, we present the main steps of the shooting method in general. Let  $y = (v, \tau, T, \phi)$ . Then one can write the system (2) in the following form

$$\frac{dy}{dz} = f(y, u), \quad \text{with } y_1(0) = 1, y_1(1) = d, y_3(0) = 1, y_4(0) = 0, \quad (4)$$

where

$$f(y, u) = \begin{pmatrix} \frac{\tau}{3\eta} \\ \text{Re} \left( \frac{1}{3\eta} v\tau - \text{Fr}^{-1} + C_1 v^{\frac{5}{2}} \right) \\ -C_2 \frac{(T-T_\infty)}{\sqrt{v}} + \frac{\Delta H \phi_\infty}{T_0 C_p} \vartheta \\ \frac{K_{max} L}{v_0} \left( \frac{1-\phi}{v} \right) \exp \left[ -4 \ln 2 \left( \frac{T-T_{max}}{D} \right)^2 \right] \end{pmatrix},$$

and  $\vartheta$  is given as follows:

$$\vartheta = \frac{K_{max} L}{v_0} \left( \frac{1-\phi}{v} \right) \exp \left[ -4 \ln 2 \left( \frac{T-T_{max}}{D} \right)^2 \right].$$

Let us make an initial guess  $s$  for  $y_2(0)$  and denote by  $y(z; s)$ , the solution of the initial value problem

$$\frac{dy}{dz} = f(y, u), \quad \text{with } y_1(0) = 1, y_2(0) = s, y_3(0) = 1, y_4(0) = 0. \quad (5)$$

Now we introduce a new dependent variable

$$x(z; s) = \frac{\partial y}{\partial s}$$

and define the second system as follows

$$\frac{\partial x}{\partial z} = \left( \frac{\partial f}{\partial y} \right) x \quad \text{with } x_1(0; s) = 0, x_2(0; s) = 1, x_3(0; s) = 0, x_4(0; s) = 0. \quad (6)$$

The solution  $y(z; s)$  of the initial value problem (5) coincides with the solution  $y(z)$  of the boundary value state system (4) provided that the value  $s$  can be found such that

$$\varphi(s) = y_1(1; s) - d = 0.$$

Using the system (6),  $\phi'(s)$  can be computed as follows

$$\phi'(s) = x_1(1; s).$$

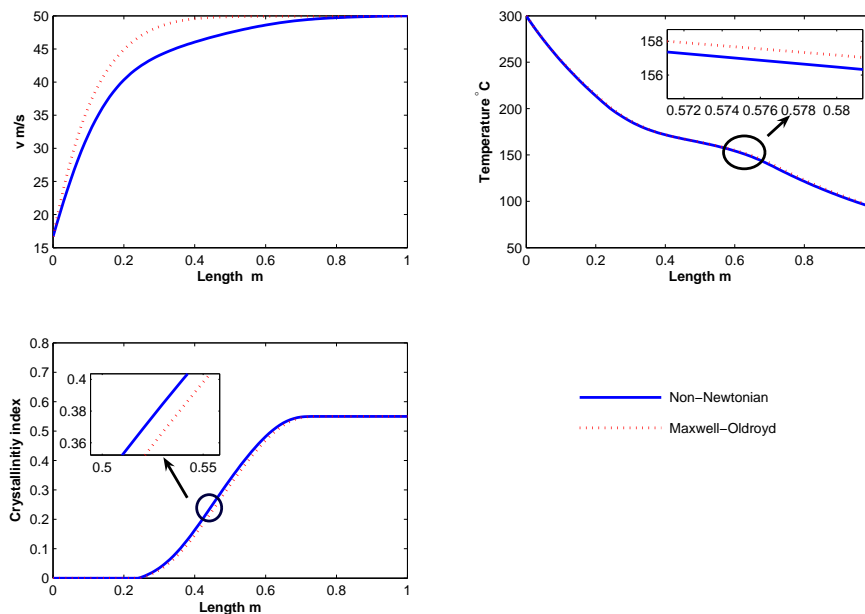
Now, using Newton–iteration, a sequence  $(s_n)_{n \in \mathbb{N}}$  is generated by

$$s_{n+1} = s_n - \frac{\phi(s_n)}{\phi'(s_n)} \quad \text{for a given initial guess } s_0.$$

If the initial guess  $s_0$  is a sufficiently good approximation to the required root of  $\phi(s) = 0$ , the theory of the Newton–iteration method ensures that the sequence  $(s_n)_{n \in \mathbb{N}}$  converges to the root  $s$ . By rearranging the system (3), the function  $f(y, u)$  can be obtained for the Maxwell-Oldroyd model.

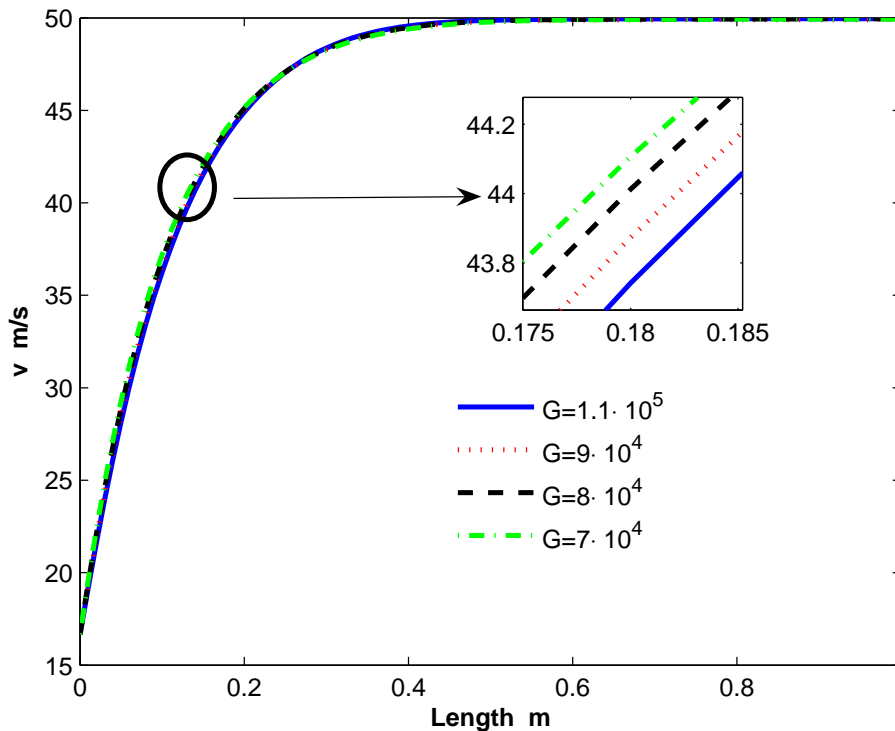
### 4.3. Results

Figure 2 shows the spinline velocity, temperature profile and crystallinity index of the non-Newtonian and Maxwell-Oldroyd models. Concerning the temperature profile, one sees a jump in the temperature owing to the heat released due to crystallization. Further, the behaviour of the temperature and crystallinity profiles are close in both cases.



**Figure 2** Spinline velocity profile(up-left), spinline temperature (up-right) profile, Crystallinity index (down-left).

Figure 3 shows the velocity profile of the Maxwell-Oldroyd model depending on the fluid shear modulus. From this one sees the the velocity profile of the melt spinning process



**Figure 3** Velocity profile depending on fluid shear modulus (pa).

has no significant variation with respect to the fluid shear modulus. But in the simulation process we experienced difficulties when the fluid shear modulus decreased. We noticed that it is needed to use higher initial guesses for the stress variable for the lower value of the fluid shear modulus. Figure 4 visualizes the final velocity vs the initial guess for stress in different fluid shear modulus. One sees from this that for a particular fluid shear modulus value, the final velocity approaches a fixed value. For example, if we consider  $G = 4 \cdot 10^4$  pa, then the final velocity approaches 38 m/s. In other words, in this case (i.e.  $G = 4 \cdot 10^4$  pa) if we set the final velocity as 50 m/s then theoretically ODE system cannot be solved. The fluid shear modulus is related to the characteristic relaxation time; lower  $G$  yields higher  $\lambda$ . We can expect this behaviour since the Maxwell-Oldroyd model (without the crystallization process) has an upper bound for the final take-up velocity which depends on the characteristic relaxation time (see (7)). This means that the flow induced crystallization Maxwell-Oldroyd model also has an upper bound for the final take-up velocity.

## 5. Conclusions

We compared the velocity, temperature and crystallization index profiles of the flow induced crystallization melt spinning process using non-Newtonian and Maxwell-Oldroyd models. The quantitative behaviour of the Maxwell-Oldroyd case is similar to the non-Newtonian case. But the qualitative behavior of the Maxwell-Oldroyd model is totally different for

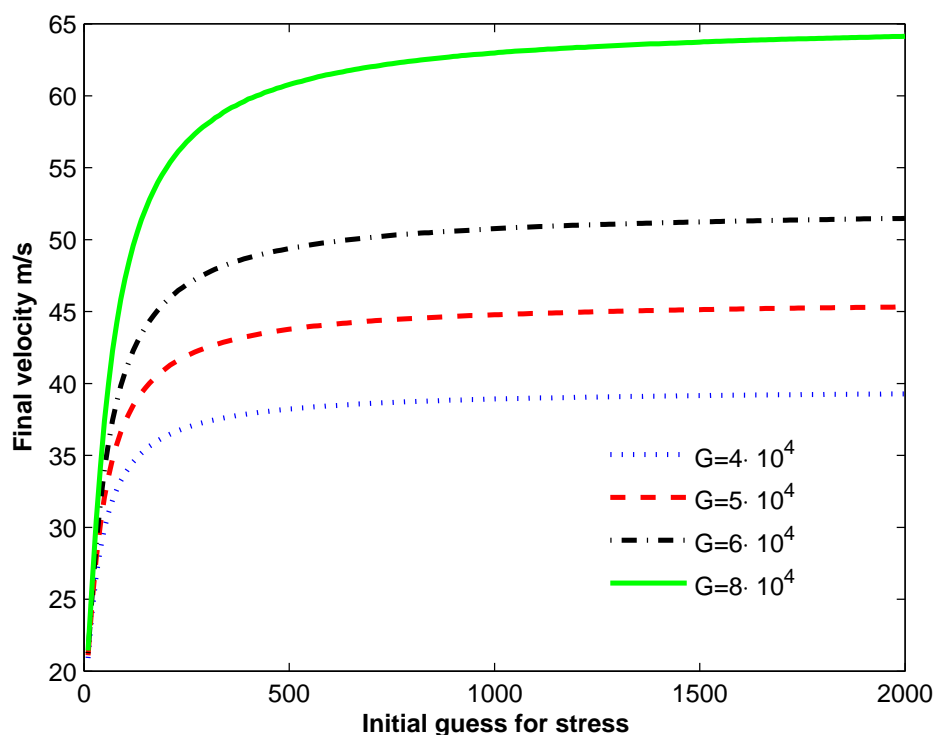


Figure 4 Final velocity depending on the initial guesses for the stress.

the lower values of the fluid shear modulus. Using numerical simulation, we have seen that the flow induced crystallization Maxwell-Oldroyd model cannot be solved with any arbitrary final velocity; i.e., The flow induced crystallization Maxwell-Oldroyd model has an upper bound for the final take-up velocity which depends on the material properties of the polymer. Theoretically, setting an arbitrary value for the final velocity may yield the spinning process unstable. Instability leads to irregular fibers or induces breakage of the individual filaments of the spinline. Clearly, this investigation is important from an industrial point of view.

## References

- [1] Bird RB, Armstrong RC, Hassager O (1987) Dynamics of Polymeric Liquids. 2<sup>nd</sup> edition, Volume 1: Fluid Mechanics, John Wiley & Sons.
- [2] Brünig H, Roland H, Blechschmidt D (1997) High Filament Velocities in the Underpressure Spunbonding Nonwoven Process. IFJ:129-134, December 1997.
- [3] Kase S, Matsuo T (1965) Studies on Melt Spinning, Fundamental Equations on the Dynamics of Melt Spinning. J. Polym. Sci. Part A 3: 2541-2554.
- [4] Langtangen HP (1997) Derivation of a Mathematical Model for Fiber Spinning. Department of Mathematics, Mechanics Division, University of Oslo, December 1997.

- 
- [5]Lee JS, Jung HW, Hyun JC, Seriven LE (2005) Simple Indicator of Draw Resonance Instability in Melt Spinning Processes. *AIChE J.*, Vol. 51, No. 10:2869-2874.
- [6]Lee JS, Shin DM, Jung HW, Hyun JC (2005) Transient Solution of the Dynamics in Low-Speed Fiber Spinning Process Accompanied by Flow-induced Crystallization. *J. Non-Newtonian Fluid Mech.* 130:110-116.
- [7]Perera SSN (2008) Phase-Space Analysis of Melt Spinning Processes, *Nihon Reoroji Gakkaishi*, Vol: 36 No. 4:161-166.
- [8]Perera SSN (2009) Viscoelastic Effect in the Non-Isothermal Melt Spinning Processes, *Applied Mathematical Sciences*, Vol: 3 No: 4: 177-186.
- [9]Shampine LF, Reichelt MW (1997) The MATLAB ODE Suite. *SIAM J. Sci. Comput.*, Vol: 18:1-22.
- [10]Ziabicki A (1976) *Fundamentals of Fiber Formation*. Wiley-Interscience, New York.